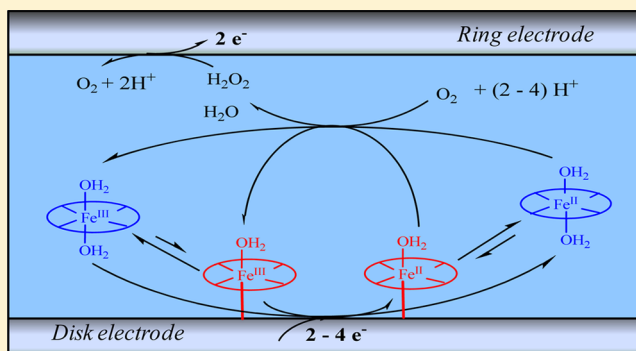# Molecular Catalysis of O$_2$ Reduction by Iron Porphyrins in Water: Heterogeneous versus Homogeneous Pathways

Cyrille Costentin,* Hachem Dridi, and Jean-Michel Savéant*

Sorbonne Paris Cité, Laboratoire d'Electrochimie Moléculaire, Unité Mixte de Recherche Université − CNRS No. 7591, Université Paris Diderot, Bâtiment Lavoisier, 15 rue Jean de Baïf, 75205 Cedex 13 Paris, France

S *Supporting Information*

ABSTRACT: Despite decades of active attention, important problems remain pending in the catalysis of dioxygen reduction by iron porphyrins in water in terms of selectivity and mechanisms. This is what happens, for example, for the distinction between heterogeneous and homogeneous catalysis for soluble porphyrins, for the estimation of H$_2$O$_2$/H$_2$O product selectivity, and for the determination of the reaction mechanism in the two situations. With water-soluble iron tetrakis(*N*-methyl-4-pyridyl)porphyrin as an example, procedures are described that allow one to operate this distinction and determine the H$_2$O$_2$/H$_2$O product ratio in each case separately. It is noteworthy that, despite the weak adsorption of the iron(II) porphyrin on the glassy carbon electrode, the

contribution of the adsorbed complex to catalysis rivals that of its solution counterpart. Depending on the electrode potential, two successive catalytic pathways have been identified and characterized in terms of current−potential responses and H$_2$O$_2$/H$_2$O selectivity. These observations are interpreted in the framework of the commonly accepted mechanism for catalytic reduction of dioxygen by iron porphyrins, after checking its compatibility with a change of oxygen concentration and pH. The difference in intrinsic catalytic reactivity between the catalyst in the adsorbed state and in solution is also discussed. The role of heterogeneous catalysis with iron tetrakis(*N*-methyl-4-pyridyl)porphyrin has been overlooked in previous studies because of its water solubility. The main objective of the present contribution is therefore to call attention, by means of this emblematic example, to such possibilities to reach a correct identification of the catalyst, its performances, and reaction mechanism. This is a question of general interest, so that reduction of dioxygen remains a topic of high importance in the context of contemporary energy challenges.

1. INTRODUCTION

Molecular catalysis of the electrochemical reduction of dioxygen (oxygen reduction reaction, ORR) has been the object of intense research activity for a very long time and continues to attract active attention presently, in resonance with the biological importance of O$_2$ reduction and in electrochemical applications such as fuel cells.[1−3] Metalloporphyrins have been extensively used for this purpose,[4] notably iron porphyrins, in very recent studies.[5,6]

While many iron porphyrins that are used as ORR catalysts in nonaqueous organic solvents are soluble and accordingly work as homogeneous catalysts, this is not the case in water, where most studies concern molecules absorbed onto the electrode surface, usually a carbon electrode, due to their low solubility.[4] The water-soluble iron tetrakis(*N*-methyl-4-pyridyl)porphyrin (FeTMPyP, Chart 1) offers an interesting example where an ORR homogeneous catalysis could be investigated in water. However, solubility in water does not a priori preclude some adsorption and therefore the interference of heterogeneous catalysis. It has been reported that the situation depends on the nature of the particular carbon used as electrode material.[7,8]

Chart 1
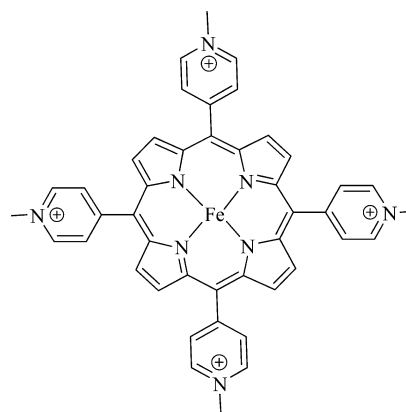
Adsorption would occur on HOPG (highly oriented pyrolytic graphite) but not on GC (glassy carbon). We have found that the

catalytic current due to adsorption of FeTMPyP on GC is not negligible, being of the same order of magnitude as the homogeneous catalytic contribution to the current. This situation requires separation of the two contributions in order to be able to estimate the H_2O_2/H_2O selectivity and to determine the kinetic characteristics of the two catalytic pathways. As a preliminary, it was necessary to select the pH of the solution to avoid dimerization of the FeTMPyP molecule. Cyclic voltammetry was used in the latter purpose as well as for mechanistic investigations. These were also carried out using rotating disk electrode voltammetry (RDEV), while rotating ring disk electrode voltammetry (RRDEV) was the main tool for estimating the H_2O_2/H_2O selectivity. One difficulty in the application of these techniques is the scarce solubility of dioxygen in water (1.4 mM at 20 °C[9]), which restrains the conditions in which the current−potential response is not merely governed by oxygen diffusion.

Instrumentation and procedures for the application of these techniques are described in detail in the Supporting Information (SI).

2. RESULTS

2.1. Current−Potential Responses of the Catalyst Alone. How To Avoid the Interference of Dimers. Figure 1a shows the reversible cyclic voltammetry (CV) of $Fe^{III}TMPyP$ in Britton−Robinson buffer (see SI) as a function of pH. A Pourbaix diagram (apparent standard potential vs pH) can thus be derived from the variation of the middle potential between the cathodic and anodic peaks, as represented in Figure 1b. According to previous electrochemical and spectrochemical studies,[7,10] the Pourbaix diagram responds to the equilibriums shown in Scheme 1, which include the formation of μ-oxo dimers. The satisfactory fitting of the Pourbaix diagram (thick line in Figure 1b) with the thermodynamic constants values listed in the caption of the figure confirms the validity of Scheme 1 as opposed to simple proton-coupled electron transfer schemes (thin lines). It also allowed the calculations of the concentrations of the various monomeric and dimeric species present as a function of pH (see SI), leading to Figure 1c.

We accordingly selected pH 3.8 to carry out most of the following experiments because the solution then contains essentially the acid form of the iron(III) monomer (Figure 1d), and the reactions in which it could be involved are at equilibrium, as shown by the proportionality of the cathodic peak to the square root of the scan rate (Figure 1d,e). Likewise, the plateau currents of the RDE voltammograms show proportionality to the porphyrin concentration (Figure 1f,g).

2.2. Current−Potential Responses of the Catalyst Alone. Is FeTMPyP Adsorbed on Glassy Carbon? As indicated previously,[8] adsorption of FeTMPyP on GC is weak. We felt, however, that is was useful to consider this point further, as it could be possible for the catalysis by the adsorbed catalyst to be nevertheless significant compared to its homogeneous counterpart if the Fe^{II} porphyrin is a more active catalyst in the adsorbed state in solution. As seen in Figure 2a, a more careful examination of the FeTMPyP cyclic voltammetry reveals that a small prewave, which we have neglected so far, is present at the foot of the large diffusion wave. This prewave may be assigned to an adsorbed Fe^{III}/Fe^{II} couple, with the Fe^{II} form being more strongly adsorbed than the Fe^{III} form.[11] This is confirmed by experiments in which the GC electrode is dipped in a pH 3.8, 0.4 M acetate buffer with $Fe^{III}TMPyP$ present during a few minutes, then pulled out, washed with the same buffer solution, and
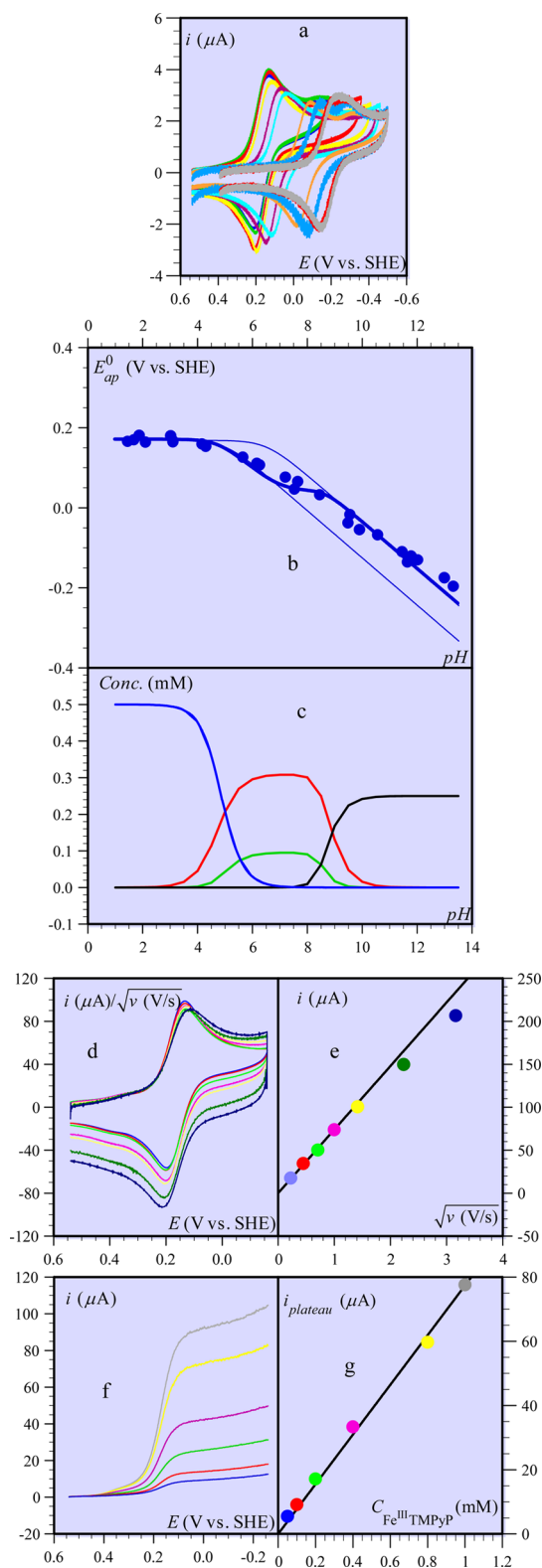

Figure 1. (a) CV under argon of 0.5 mM $Fe^{III}TMPyP$ in 0.04 M Britton−Robinson buffer as a function of pH on a 3 mm diameter GC electrode at 0.1 V/s (from left to right: pH = 1.7, 2.1, 3, 4.3, 6.1, 7.1, 10, 11.65, 13.0, 13.4). (b) Pourbaix diagram obtained by plotting pH against the midpoints between cathodic and anodic peak potentials of the first wave of the CVs shown in (a), with additional data points derived from CVs not shown in (a) for clarity. Thin lines: fitting for a simple ET−PT scheme with $E^0_{OH^-} = 0.18$ V vs SHE; $pK^{III}_a = 5$ (left) and 6.5 (right). Thick line: fitting according to Scheme 1 for $E^0_{OH^-} = 0.18$ V vs SHE; $pK^{III}_a = 5$,

Figure 1. continued

$pK_a^{III} = 7$, $K_D^{OH_2} = 10^3$ $(M^{-1/2})$,[7,10] $pK_a^{III-O-III} = 8.5$. (c) Concentrations of $H_2O-Fe^{III}-OH_2$ (blue), $H_2O-Fe^{III}-{}^-OH$ (red), $H_2O-Fe^{III}-O-Fe^{III}-OH_2$ (green), $HO^--Fe^{III}-O-Fe^{III}-{}^-OH$ (black). (d) CV under argon of 1 mM $Fe^{III}TMPyP$ in a 0.4 M acetate buffer + 0.1 M KNO_3 at pH 3.8 on a 5.6 mm diameter GC electrode; scan rate (V/s): 0.05 (blue), 0.2 (red), 0.5 (light green), 1 (magenta), 2 (yellow), 5 (dark green), 10 (dark blue). (e) Variation of the peak current in (d) with the scan rate. (f) RDE voltammograms of $Fe^{III}TMPyP$ at 2500 rpm in a 0.4 M acetate buffer + 0.1 M KNO_3 at pH 3.8 on a 5.6 mm diameter GC electrode as a function of concentration from top to bottom: 1, 0.8, 0.4, 0.2, 0.1, 0.05 mM. (g) Plateau current vs concentration.
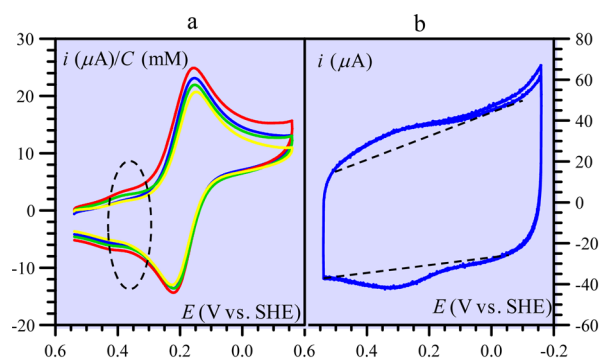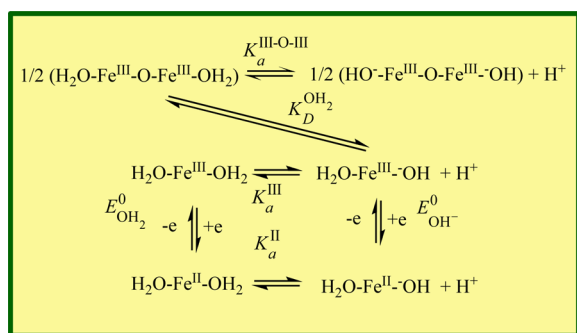
Scheme 1

Figure 2. (a) CV under argon of $Fe^{III}TMPyP$ in a pH 3.8, 0.4 M acetate buffer + 0.1 M KNO_3 as a function of concentration (C) of $Fe^{III}TMPyP$ at 0.05 V/s on a 5.6 mm GC electrode ($C = 1, 0.8, 0.4, 0.2$ mM). (b) CV of a GC electrode dipped in a 1 mM solution of $Fe^{III}TMPyP$ in a pH 3.8, 0.1 M acetate buffer during 3 min, then pulled out, washed with the same buffer solution, and transferred into a fresh buffer solution of the same composition with no $Fe^{III}TMPyP$ present. Scan rate: 5 V/s.

transferred into a fresh buffer solution of the same composition with no $Fe^{III}TMPyP$ present, showing a small adsorption wave in the same potential range (Figure 2b). This evidence of an adsorption of the $Fe^{III/II}TMPyP$ couple will be taken into account in the discussion of the catalysis kinetics, based on a rough estimate of the amount of catalyst adsorbed, $\Gamma^0 = 2 \times 10^{-11}$ M/cm^2, as sketched in Figure 2b.

2.3. Reduction of O_2 Alone on the Same GC Electrode and in the Same Buffer (pH 3.8). The investigation of O_2 alone on the same GC electrode in the same buffer was deemed necessary to estimate the potential range where the catalytic reduction can be carried out with negligible interference of the direct reduction at the electrode (Figure 3a). It was also the occasion of determining the H_2O_2/H_2O product selectivity of O_2 reduction at this pH by use of the RRDEV device (Figure 3b,c).
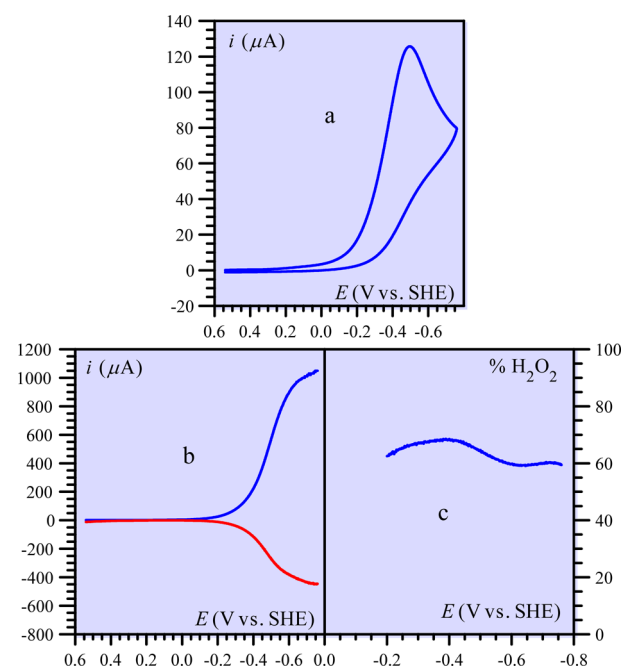

Figure 3. (a) CV under 1 atm O_2 in a pH 3.8, 0.4 M Britton−Robinson buffer at 0.05 V/s on a 5.6 mm GC electrode. (b) RRDEV of the same solution at 2500 rpm and 0.05 V/s; blue curve, disk current as a function of potential; red curve, ring current/N_{eff} as a function of the disk potential when the ring potential is poised at 1.04 V vs SHE. (c) Percentage of H_2O_2 formed (see text).

The apparent number of electrons exchanged, n_{ap}, and the percentage of H_2O_2 formed can be derived from the disk and ring current, i_{disk} and i_{ring}, according to the following equations (assuming no direct reduction of H_2O_2 at the disk electrode).[12a]

$$\%H_2O_2 = 100\frac{\frac{2i_{ring}}{N_{eff}}}{i_{disk} + \frac{i_{ring}}{N_{eff}}}, \quad n_{ap} = \frac{4i_{disk}}{i_{disk} + \frac{i_{ring}}{N_{eff}}} \text{ and}$$

$$\%H_2O_2 = 100\frac{4 - n_{ap}}{2}$$

where N_{eff} is the collection efficiency.[12] In the potential range where enough H_2O_2 is produced for a reasonably accurate determination to be possible, $\%H_2O_2 \approx 60$ and $n_{ap} = 2.8$.

2.4. Catalysis of O_2 Reduction by $Fe^{II}TMPyP$. General Features. Figure 4a shows the RDE catalytic voltammograms as a function of the rotation rate as compared to the voltammogram for the direct reduction of O_2 obtained at the highest rotation rate. There is a good separation in potential of the catalytic and direct reductions, thus allowing a detailed examination of the former process. Figure 4a,b shows that the current tends to vary proportionally to the square root of the rotation rate upon going to negative potentials, pointing to kinetic control by O_2 diffusion.[13] Conversely, it is almost independent from the rotation rate at the foot of the catalytic wave, indicating kinetic control by the catalytic reaction.[13]

We also note that the catalytic limiting current (blue curve in Figure 4a) is larger than the O_2 direct reduction-limiting current (black curve in Figure 4a) at the same rotation rate (2500 rpm), indicating that the electron stoichiometry is larger in the first case than in the second. It follows that the H_2O_2/H_2O product ratio in the catalyzed reduction is smaller than that in the direct reduction. This is confirmed by the RRDEV experiments shown
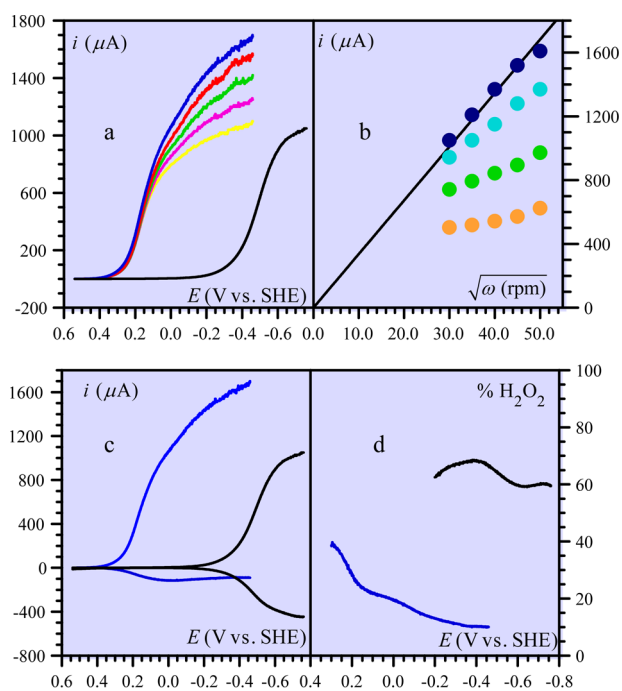
Figure 4. (a) RDEV of 1 mM Fe^{III}TMPyP on a 5.6 mm GC electrode under 1 atm O_2 in a pH 3.8, 0.4 M acetate buffer + 0.1 M KNO_3 as a function of the rotation rate (rpm): 900 (yellow), 1225 (magenta), 1600 (green), 2025 (red), 2500 (blue); 1 atm O_2 alone in the same solution at 2500 rpm (black curve), $v = 0.05$ V/s. (b) Variation of the current with the square root of the rotation rate as a function of the electrode potential (V vs SHE): 0.14 (orange), 0.04 (green), −0.16 (cyan), −0.36 (dark blue). (c) RRDEV of the same solution: (top blue curve) disk current as a function of potential; (bottom blue curve) ring current/N_{eff} as a function of the disk potential when the ring potential is poised at 1.04 V vs SHE for $\omega = 2500$ rpm. In black: same curves for the direct reduction of O_2 (recall Figure 3b). (d) Apparent percentage of H_2O_2 formed.
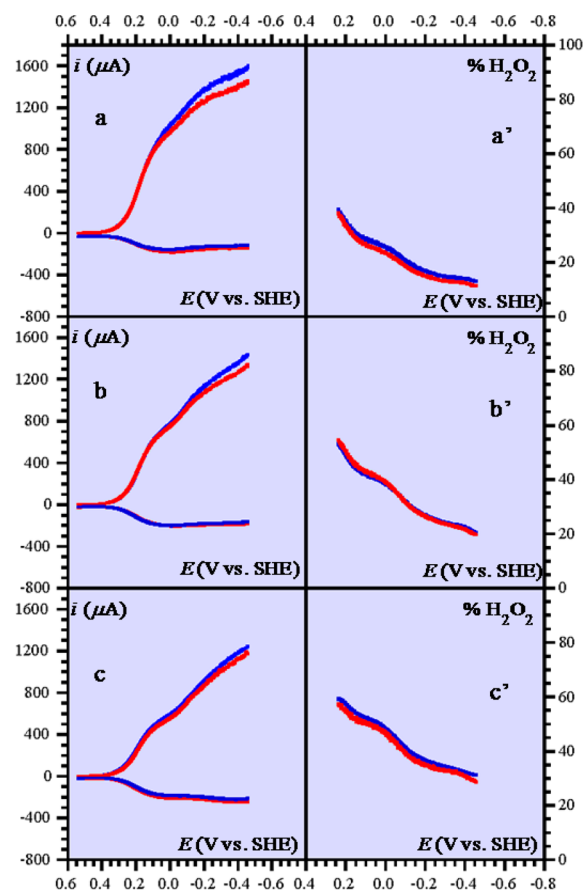

Figure 5. (a−c) RRDEV of Fe^{III}TMPyP on a 5.6 mm GC electrode under 1 atm O_2 in a pH 3.8, 0.4 M acetate buffer as a function of the catalyst concentration (mM): (a) 0.8, (b) 0.4, and (c) 0.2 at 2500 (blue) and 2025 (red) rpm; (top curves) disk current as a function of potential; (bottom curves) ring current/N_{eff} as a function of the disk potential when the ring potential is poised at 1.04 V vs SHE. (a′−c′) Percentage of H_2O_2 formed under the same conditions.

in Figure 4c that shows that the catalytic ring current is smaller than the direct reduction ring current.

Another important feature of the catalytic responses is that they are actually composed of two successive waves, as more clearly appears upon decreasing the catalyst concentration (Figure 5a−c). The first wave is under complete kinetic control by the catalytic reaction as follows from the independence of the current with respect to the rotational speed. It is also worth noting that the apparent H_2O_2/H_2O product ratio is smaller at the second wave than at the first.

It is seen that at the foot of the catalytic wave the apparent H_2O_2/H_2O product ratio rapidly drops. As shown later, this is due to the fact that the foot of the catalytic wave is mainly due to heterogeneous catalysis, which leads to a H_2O_2/H_2O product ratio higher than that for homogeneous catalysis.

A note of caution regarding the determination of product selectivity ratio H_2O_2/H_2O from the RRDEV ring/disk current ratio is needed. Indeed, during their travel from the disk, where they are generated, to the ring where they are detected, H_2O_2 molecules may undergo side reactions that will minimize their production by the catalytic reaction taking place at the disk. One notable such side reaction is the disproportionation of H_2O_2 triggered by Fe^{III}TMPyP. The rate constant of this reaction is 10 M^{-1} s^{-1} in acidic media,[10a] meaning that for 1 mM Fe^{III}TMPyP, the pseudo-first-order rate constant is 10^{-2} s^{-1}. In a typical RRDEV setup, similar to the one we have used (see SI), the

collection efficiency in the presence of a coupled first-order reaction, N_{eff}^k, is given by[14]

$$N_{eff}/N_{eff}^k = 1 + 1.28 v/D_{H_2O_2}^{1/3}(k/\omega)$$

where v is the viscosity of water (10^{-2} cm^2/s[15]), $D_{H_2O_2} = 1.7 \times 10^{-5}$ cm^2/s, the diffusion coefficient of H_2O_2,[15] and k is the first-order rate constant. At a rotation rate of $\omega = 2500$ rpm, as mostly used in this work, $N_{eff}/N_{eff}^k = 1.0024$, meaning that this reaction may be ignored in the following data treatment. This is not a priori the case for the possible reduction of H_2O_2 by the Fe^{II}TMPyP complex generated at the disk electrode, as will be discussed in the following sections.

2.5. Catalysis of O_2 Reduction by Adsorbed FeTMPyP (Heterogeneous Catalysis). We have seen, in section 2.2, that Fe^{III}TMPyP is weakly adsorbed on the GC electrode. Despite this modest adsorption, does the corresponding heterogeneous catalysis contribute significantly to the overall catalytic process is the question we address now. The answer is given by the experiments summarized in Figure 6 and described in the caption of this figure. It appears that the contribution of the heterogeneous process to the overall catalysis is by no means negligible, with the corresponding current being on the order of one-half of the total (compare Figure 6 with Figures 4 and 5). We also note that the H_2O_2/H_2O product ratio is larger than that in
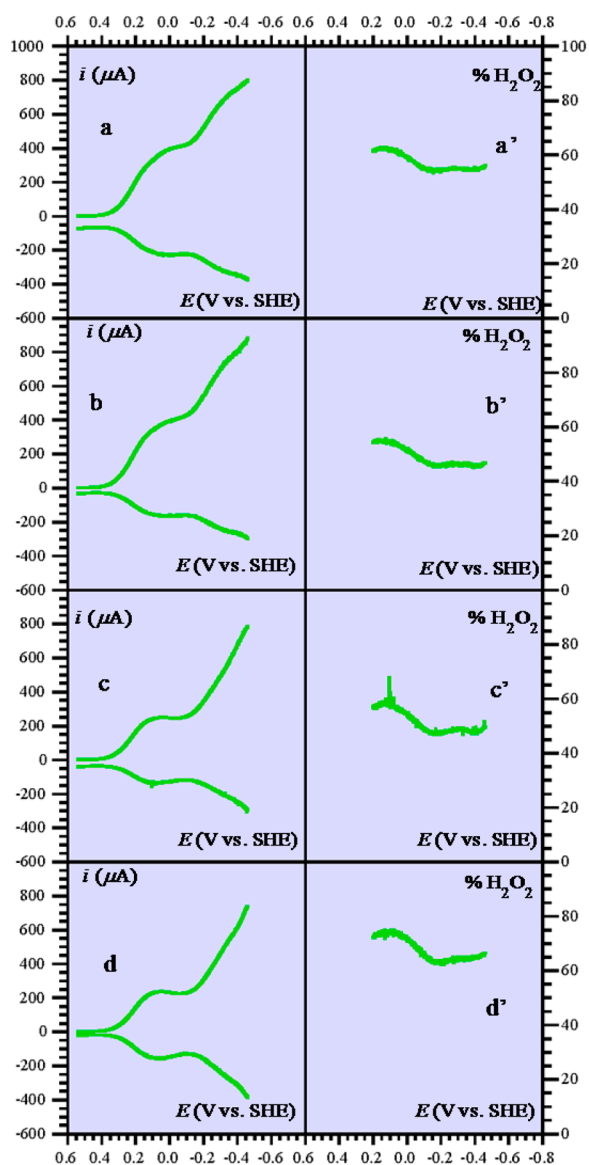
Figure 6. (a–d) RRDEV under 1 atm O_2 of a 5.6 mm GC electrode dipped in solutions of $Fe^{III}TMPyP$ in a pH 3.8, 0.4 M acetate buffer during 15−20 min to reach the saturation adsorption corresponding to the solution concentration, then pulled out, washed with the same buffer solution, and transferred into a fresh buffer solution of the same composition with no $Fe^{III}TMPyP$ present. $Fe^{III}TMPyP$ concentrations (mM): 1 (a), 0.8 (b), 0.4 (c), 0.2 (d). Rotation rate: 2500 rpm; $v = 0.05$ V/s. Bottom curves: ring current/N_{eff} as a function of the disk potential when the ring potential is poised at 1.04 V vs SHE. (a′−d′) Percentage of H_2O_2 formed under the same conditions.
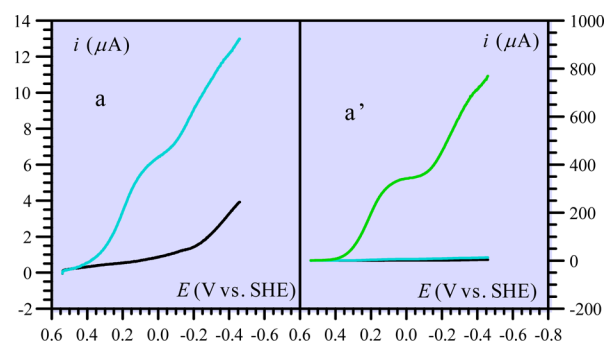

Figure 7. RDEV of a 5.6 mm GC electrode dipped in solutions of $Fe^{III}TMPyP$ in a pH 3.8, 0.4 M acetate buffer during 10 min to reach the saturation adsorption corresponding to the solution concentration, then pulled out, washed with the same buffer solution, and transferred into a fresh buffer solution of the same composition with no $Fe^{III}TMPyP$ present. Black curve: neither O_2 nor H_2O_2 present. Cyan curve: 1 mM H_2O_2 present in solution. Green curve: under 1 atm O_2.

the global catalysis process, being close to its value for the direct O_2 reduction.

Does all of the H_2O_2 produced at the disk electrode in the experiments of Figure 6 reach the ring electrode or is part of it reduced by the $Fe^{II}TMPyP$ complex generated at the disk electrode? In other words, do the data displayed in the right part of Figure 6 reliably represent the whole of the H_2O_2 molecules produced at the disk? The answer is provided by the experiments depicted in Figure 7. $Fe^{II}TMPyP$ does catalyze the reduction of H_2O_2 produced at the disk electrode (Figure 7a) but to a negligible extent compared to the reduction of O_2 (Figure 7b).

We may therefore view the data in the right column of Figure 6 as representing reliably the H_2O_2/H_2O selectivity ratio of the heterogeneous catalytic reaction.

2.6. Homogeneous Catalysis of O_2 Reduction by $Fe^{II}TMPyP$. As seen in Figure 5, the first catalytic wave is independent of the rotation rate, indicating that there is no interference of mass transport. It may thus be considered that, within the corresponding potential range, the heterogeneous and homogeneous contributions to catalysis are additive, and the latter can be obtained by subtraction of the results of section 2.5 from those of section 2.4. The result is shown in Figure 8a−d. As appears in Figure 8e, at a given potential of the first wave (e.g., 0.04 V vs SHE), the homogeneous catalysis current varies, as expected, approximately proportionally to the catalyst concentration, whereas the heterogeneous catalysis current remains constant as anticipated from the constancy of the saturation surface concentration of the catalyst. It should be noted that the subtraction procedure does not represent the exact contribution of homogeneous catalysis at potentials more negative than the first wave.

As discussed above, the reduction of H_2O_2 is not catalyzed appreciably by adsorbed $Fe^{II}TMPyP$. In experiments where $Fe^{III}TMPyP$ is present in the solution, the reduction of H_2O_2 produced by both heterogeneous and homogeneous catalysis of O_2 reduction may, however, be catalyzed by the $Fe^{II}TMPyP$ molecules generated at the electrode, which diffuse away from the electrode. Detection at the ring will miss these H_2O_2 molecules and thus unduly minimize the H_2O_2/H_2O product ratio. The following RDEV experiments (Figure 8f) show that $Fe^{II}TMPyP$ does catalyze the reduction of H_2O_2, and that the reaction is endowed with a rate constant equal to ca. 10^4 M^{-1} s^{-1} (see SI). This reaction is fast, but it is slower than the reduction of O_2 by $Fe^{II}TMPyP$ (Figure 8f). Pure kinetic behavior observed at a high rotation rate implies that reduction reactions are taking place within a reaction layer adjacent to the disk electrode. The thickness of this reaction layer is governed by the fastest reaction, which here is O_2 reduction (this can be inferred from the relative current for O_2 and H_2O_2 reductions in RDEV in comparable concentrations). Outside this reaction layer, H_2O_2 only diffuses and may reach the ring electrode. Consequently, the ring current is relative to the amount of H_2O_2 escaping the reaction layer. The size of this reaction layer is much smaller than the distance between the disk electrode and the ring electrode. Therefore, the
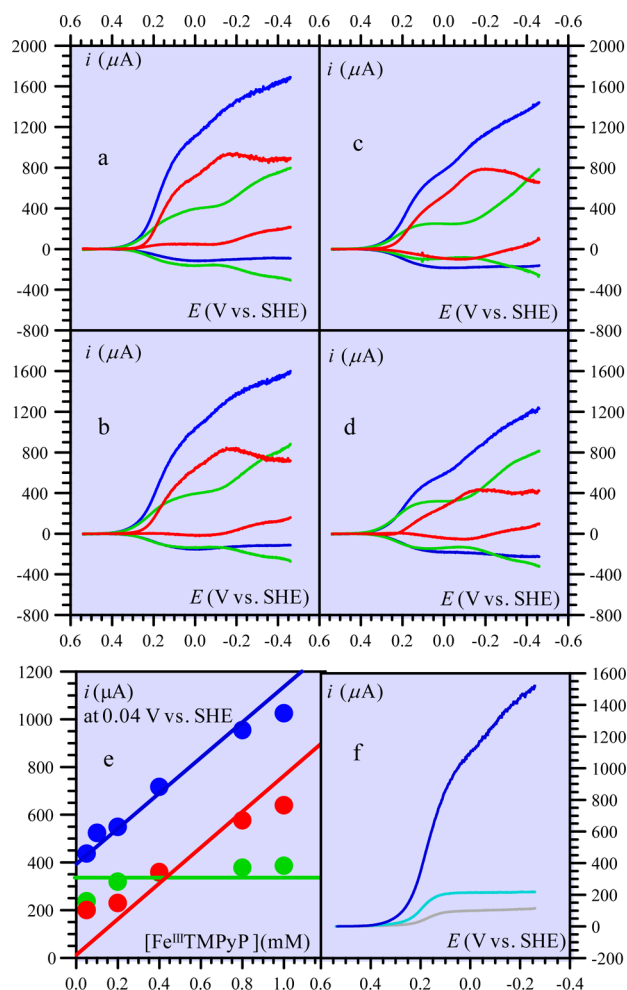
Figure 8. (a−d) Construction of the homogeneous catalysis RRDEV responses under 1 atm O_2 (red curves) by the difference between the global catalysis responses (blue curves as in Figures 4c and 5a−c) and the heterogeneous catalysis RRDEV responses (green curves as in Figure 6); $Fe^{III}TMPyP$ concentrations (mM): 1 (a), 0.8 (b), 0.4 (c), 0.2 (d). Rotation rate: 2500 rpm. (e) Current at 0.04 V vs SHE vs catalyst concentration for global catalysis (blue dots), heterogeneous catalysis (green dots), and homogeneous catalysis (red dots). (f) REDV at 2500 rpm of 1 mM $Fe^{III}TMPyP$ in a pH 3.8, 0.4 M acetate buffer under argon (gray), in the presence of 1 mM H_2O_2 (cyan) and under 1 atm O_2 (blue).

Figure 9. RRDEV of a 0.2 mM solution $Fe^{III}TMPyP$ in a pH 3.8, 0.4 M acetate buffer (rotation rate: 2500 rpm) (a) under 1 atm O_2 (blue curves, global catalysis; green curves, heterogeneous catalysis as in Figure 6; red curves, homogeneous catalysis obtained by the difference between the blue and green curves); (b) in air (magenta curves, global catalysis; gray curves obtained as in (a) but in air instead of 1 atm O_2; orange curves, homogeneous catalysis obtained by difference between the magenta and gray curves). (c) Heterogeneous catalysis under 1 atm O_2 (green as in a) and air (gray as in b, dotted gray: ×5). (d) Homogeneous catalysis under 1 atm O_2 (red curve as in a) and air (orange as in b, dotted orange: ×$\sqrt{5}$).

H_2O_2 molecules effectively collected at the ring, i_{ring}/N_{eff}, are related to the flux that escapes the reaction layer. Determination of the fraction of H_2O_2 that escapes reduction of H_2O_2 in the reaction layer requires knowing the mechanism. This is the reason that analysis of H_2O_2/H_2O selectivity for the homogeneous catalysis is postponed after a mechanism is proposed, which requires examining first the effects of O_2 concentration and pH on the catalytic current.

2.7. Effect of O_2 Concentration. The effect of dioxygen concentration on the heterogeneous and homogeneous catalysis is examined by comparison of the RDEV and RRDEV curves obtained under 1 atm O_2 (Figure 9a) and air (Figure 9b). The amount of H_2O_2 formed, as reflected by the ring current, is almost entirely due to the heterogeneous processes in both cases (Figure 9a,b). The corresponding selectivity is ca. 55% H_2O_2 under O_2 and 50% H_2O_2 under air.

The heterogeneous catalysis disk current is clearly dependent on the O_2 concentration (Figure 9c). It varies less than
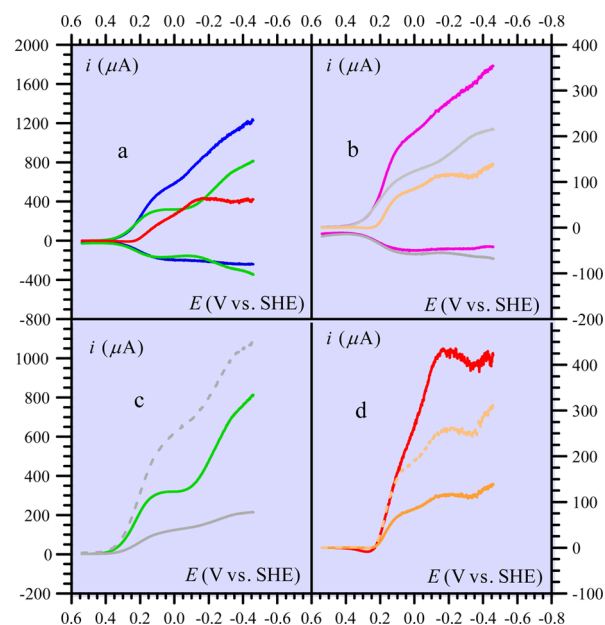
proportionally to $[O_2]$. This observation indicates that the addition of O_2 on the Fe^{II} porphyrin, although it clearly interferes in the catalysis kinetics, is neither the rate-determining step nor a pre-equilibrium of the rate-determining step.

Assuming, as above, the additivity of the heterogeneous and homogeneous contributions, the latter is obtained by subtraction of the former from the global catalysis response, leading to the red and orange curves in Figure 9a,b and in Figure 9d. The first wave current is proportional to $\sqrt{[O_2]}$, indicating that the addition of O_2 on the Fe^{II} porphyrin is either the rate-determining step or a pre-equilibrium of the rate-determining step.[16] This assertion also falls in line with the observation that the half-wave potential is equal to the standard potential of the Fe^{III}/Fe^{II} couple.[16c] At a potential more negative than −0.1 V, O_2 mass transport starts to interfere significantly. The variation of the current with O_2 concentration is then more important than proportionality to $\sqrt{O_2}$, thus explaining why an apparent increase of the reaction order with respect to O_2 is observed.

2.8. Dependence toward pH. The previous RRDEV experiments were repeated at a pH of 1.15 in order to gauge the effect of pH on the kinetics of catalysis and on the H_2O_2/H_2O selectivity ratio.[17] It is seen (Figure 10) that there is practically no effect of pH on the heterogeneous and homogeneous catalytic RDEV waves. The same is true for the RRDEV waves, indicating that the H_2O_2/H_2O selectivity ratio does not vary appreciably in this pH range.

3. DISCUSSION

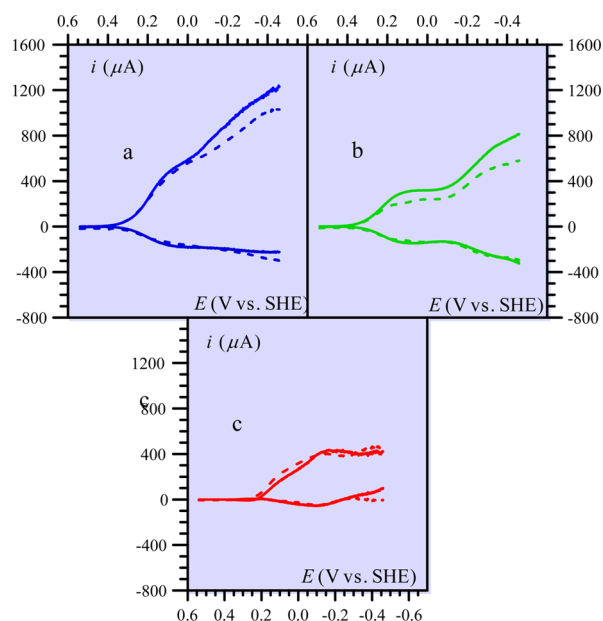The most striking of our observations, at variance with previous reports,[8,10] is that the $Fe^{III/II}TMPyP$ couple catalyzes O_2

Figure 10. RRDEV (rotation rate: 2500 rpm) of a 0.2 mM solution Fe^{III}TMPyP at pH 3.8, 0.4 M acetate buffer (solid line) and pH 1.15 (dashed line) under 1 atm O$_2$. (a) Global catalysis. (b) Heterogeneous catalysis. (c) Homogeneous catalysis.

reduction not only in solution but also at the adsorbed state when using glassy carbon as the electrode material. In spite of the weak adsorption of both members of the couple, the contributions of heterogeneous and homogeneous catalysis are of similar magnitude. An analysis of the kinetics of the two catalytic regimes is required to know whether this observation is related either to an intrinsic difference of reactivity or to the involvement of different amounts of catalytic material in the two cases or to a combination of these two factors. Before addressing this point, it is worth summarizing the characteristics of each of the two catalytic regimes to establish the reaction sequence they entail. We note in this regard that the second important finding of the present study is that both heterogeneous and homogeneous catalysis regimes give rise to two successive waves. In both cases, the first of these occurs around the standard potential of the Fe$^{III/III}$TMPyP couple. The second, more negative, wave is likely to involve the reduction of an intermediate formed at the first wave.

The main characteristics of the heterogeneous catalytic process are (i) the O$_2$ reaction order at the first wave is less than 1; (ii) the pH has no noticeable effect on the first wave; (iii) selectivity is ca. 60% H$_2$O$_2$, 40% H$_2$O, independent of pH and [O$_2$]. Using the intermediate species commonly invoked in the reduction of dioxygen by Fe^{II} porphyrins,[4] these observations suggest the mechanism depicted in Scheme 2. After the initial electron transfer, which converts the starting Fe^{III} porphyrin into the Fe^{II} porphyrin, the complex resulting from the addition of O$_2$ on the latter is protonated, giving rise to the intermediate noted in red in the scheme. As in most ECE-type mechanisms driven by a protonation reaction, the resulting protonated species is easier to be reduced than the starting molecule.[18] This second E-step produces the intermediate noted in blue, which is at the crossroad of product selection for the first wave catalysis and whose reduction triggers the second catalytic wave. In the framework of these ECEC (forming H$_2$O$_2$) or ECECEE (forming H$_2$O) reaction pathways, the plateau current of the

first wave, i_{pl}, and its half-wave potential may be expressed by (see SI):

$$\frac{i_{pl}}{FS} = n_{ap}\frac{\Gamma^0}{\dfrac{1}{k_1^{het}} + \dfrac{1}{k_{2,H_2O_2}^{het} + k_{2,H_2O}^{het}}}$$ (1)

with

$$n_{ap} = 4 - 2\left(\frac{\%H_2O_2}{100}\right)$$

$$E_{1/2} = E_{cat}^0 + \frac{RT}{F}\ln\left(1 + \frac{k_1^{het}}{k_{2,H_2O_2}^{het} + k_{2,H_2O}^{het}}\right)$$ (2)

as a function of the global rate constant, k_1^{het}, of the first two steps following the initial electron transfer and of the two rate constants, $k_{2,H_2O_2}^{het}$ and k_{2,H_2O}^{het}, of the H$_2$O$_2$- and H$_2$O-forming steps, respectively (Γ^0 is the surface concentration of catalyst, and E_{cat}^0 is the standard potential of the catalyst couple). i_{pl} depends on the O$_2$ concentration but with a reaction order smaller than 1. The observation that the first wave current does not depend on pH shows that the addition of O$_2$ on the Fe^{II} porphyrin is irreversible, presumably so because of rapid protonation of the addition complex. Bond cleavages in the second C steps are likewise irreversible, possibly due to rapid follow-up protonation in this case, too. The mechanism is completed by the reduction of the blue intermediate at a more negative potential, giving rise to the green intermediate, which splits in a similar manner, although somewhat more in favor of H$_2$O$_2$.

Because the plateau current is not proportional to [O$_2$] and because the half-wave potential is not far from E_{cat}^0, we may consider that $k_1^{het} \approx k_{2,H_2O_2}^{het} + k_{2,H_2O}^{het}$ and thus that

$$\frac{i_{pl}}{FS} \approx \frac{n_{ap}}{2}k_1^{het}\Gamma^0$$ (3)

Application of eq 3 to the data displayed in Figure 8e (green dots) leads to $k_1^{het} \approx 780$ s^{-1}.

Turning now to the homogeneous catalytic process, its main characteristics are (i) the O$_2$ reaction order at the first wave is 1 and the half-wave potential is equal to the standard potential of the Fe^{III}/Fe^{II} couple; (ii) the pH has no noticeable effect on the first wave; (iii) a direct estimation of the selectivity ratio from ring/disk current ratio is not possible because reduction of H$_2$O$_2$ has to be considered.

For the same reasons as for the heterogeneous case, the mechanism sketched in Scheme 2 is applicable here, with the difference that addition of O$_2$ to the Fe^{II} complex is irreversible and rate-determining, that is, $k_1^{hom} \ll k_{2,H_2O_2}^{hom} + k_{2,H_2O}^{hom}$. The second catalytic process is triggered by the reduction of the blue intermediate, which is easier to reduce than when it is adsorbed on the electrode, presumably because of a stronger axial ligation in the adsorbed state. As already mentioned, the reduction of H$_2$O$_2$ produced both by heterogeneous and homogeneous catalysis of O$_2$ reduction is catalyzed by the Fe^{II}TMPyP molecules generated at the electrode, which diffuse away from the electrode. Detection at the ring will miss these H$_2$O$_2$ molecules and thus unduly minimize the H$_2$O$_2$/H$_2$O product ratio. However, focusing on the first wave, it can be shown that the disk current is given by (see SI)

Scheme 2
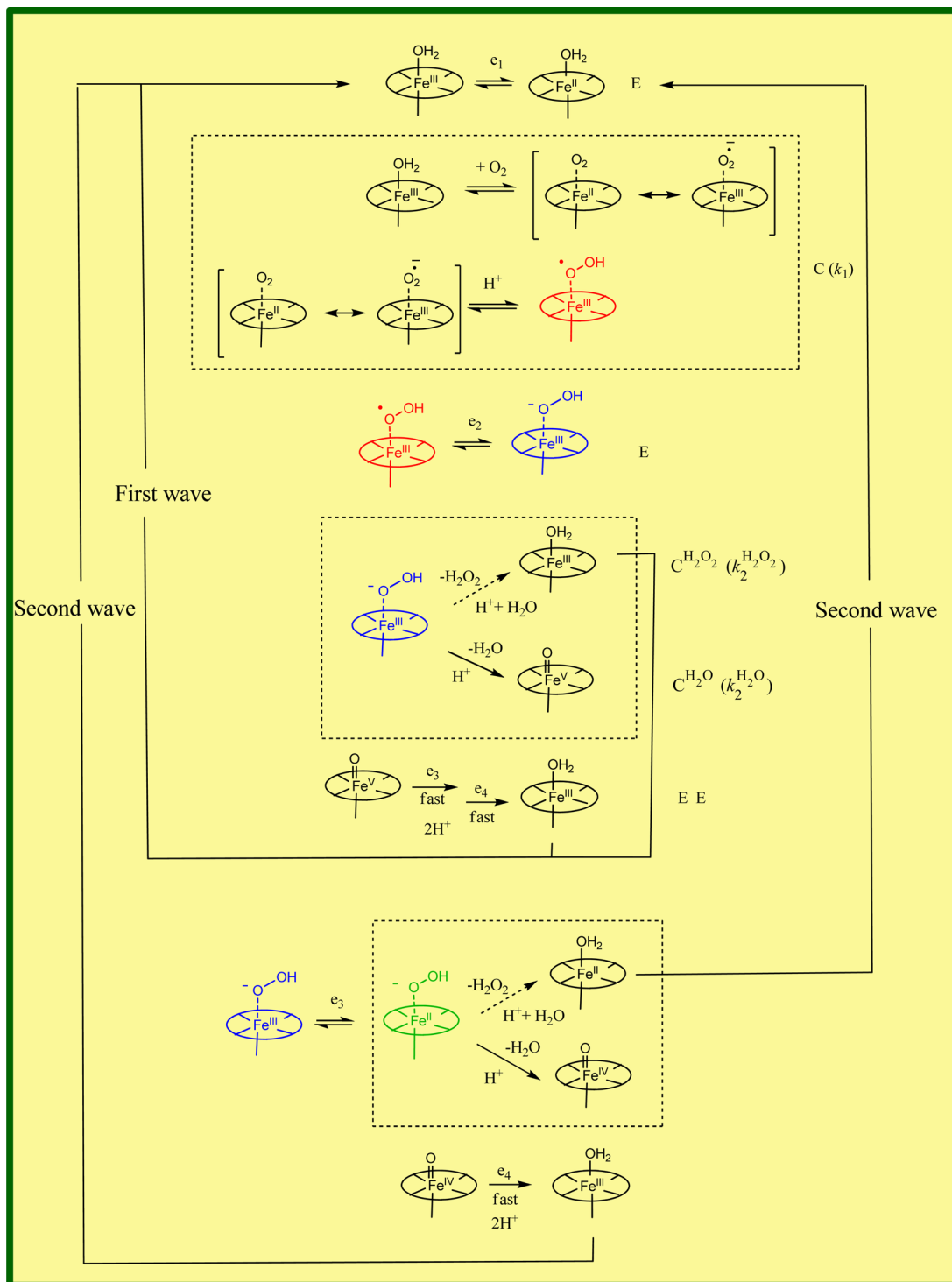
$$\frac{i}{FS} = \frac{i^{het}}{FS}$$

$$+ \frac{2\left(1 + \frac{k_{2,H_2O}^{hom}}{k_{2,H_2O_2}^{hom} + k_{2,H_2O}^{hom}} \frac{k_1^{hom}}{k_1 + k_3[H_2O_2]}\right)\sqrt{D_{cat}(k_1^{hom} + k_3[H_2O_2])}\, C_{cat}^0}{1 + \frac{\sqrt{k_1^{hom} + k_3[H_2O_2]}}{\sqrt{k_{2,H_2O_2}^{hom} + k_{2,H_2O}^{hom}}}\left(\frac{k_1^{hom}}{k_1^{hom} + k_3[H_2O_2]}\right) + \exp\left[\frac{F}{RT}(E - E^0)\right]}$$

(4)

where k_3 is the rate constant for H_2O_2 reduction by $Fe^{II}TMPyP$ and $[H_2O_2]$ the concentration of H_2O_2 in the reaction layer at a

given potential. Because it is observed experimentally that (i) the homogeneous contribution of the disk current is proportional to $\sqrt{[O_2]}$, that is, to $\sqrt{k_1^{hom}}$; and (ii) the half-wave potential is very close to E^0, and we conclude that in our experimental conditions $k_1^{hom} \gg k_3[H_2O_2]$ and $(k_1^{hom})^{1/2} \gg (k_{2,H_2O_2}^{hom} + k_{2,H_2O}^{hom})^{1/2}$. Then the plateau current for the homogeneous contribution to the disk current is

$$\frac{i_{pl}^{hom}}{FS} = n_{ap}C_{cat}^0\sqrt{D_{cat}}\sqrt{k_1^{hom}}$$

(5)

with

$$n_{ap} = 4 - 2\left(\frac{\%H_2O_2}{100}\right) \text{ and}$$

$$\left(\frac{\%H_2O_2}{100}\right) = \frac{k_{2,H_2O_2}^{hom}}{k_{2,H_2O_2}^{hom} + k_{2,H_2O}^{hom}} = \frac{\frac{2i_{ring}^{hom}}{N_{eff}}}{i_{disk}^{hom} + \frac{i_{ring}^{hom}}{N_{eff}}}$$

The ring current for the homogeneous catalysis is finally obtained by subtracting from this corrected ring current the contribution from the heterogeneous catalysis (Figure 8). It thus appears that this ring current is small and not easy to measure, indicating selectivity smaller than 20%. This estimation is very approximate and has no other merit than to indicate that the H_2O_2/H_2O selectivity ratio for homogeneous catalysis is clearly less than that for heterogeneous catalysis.

Application of eq 5 to the data displayed in Figure 8e (red dots) leads to $k_1^{hom} \approx 30 \text{ s}^{-1}$.[19] It is interesting to note that equation (5) may be rewritten as

$$\frac{i_{pl}}{FS} = n_{ap}\left(C_{cat}^0\sqrt{\frac{D_{cat}}{k_1^{hom}}}\right)k_1^{hom}$$

where $(D_{cat}/k_1^{hom})^{1/2}$ is the thickness of the catalytic reaction–diffusion layer (see SI), where the molecules that actually partake in the catalytic process are located. $C_{cat}^0(D_{cat}/k_1^{hom})^{1/2}$ is thus the surface concentration of the molecules effectively partaking in the catalytic process, to be compared with Γ^0 in heterogeneous catalysis (2×10^{-10} vs 2×10^{-11} M/cm^2).[20]

These differences between the two catalytic regimes have been taken into account in the above estimation of the rate constants; the ratio of 26 in favor of the heterogeneous pathway therefore does represent an actual and significant difference in reactivity, even though several parameters have been estimated rather crudely. A plausible interpretation of the increased efficiency of heterogeneous versus homogeneous catalysis is that it may be related to a better ligation of the complex at the adsorbed state, presumably by ligands present on the GC surface, rather than by the ligands available in solution.[21] This better ligation is expected to favor the rate formation of the initial $Fe^{II}O_2$ ($Fe^{III}O_2^{\bullet-}$)[22] and therefore catalytic efficiency. A ligation by ligands present on the GC surface better than that by the ligands available in solution may also be inferred from the fact that the standard potential of the adsorbed couple is ca. 120 mV more positive than its homogeneous counterpart.

This likely explanation of the differences and similarities between the heterogeneous and homogeneous catalysis by FeTMPyP has assumed that the same iron porphyrin molecule as in solution is adsorbed on the electrode surface, albeit with some difference in axial ligation. This assumption is based on the proximity of the standard potentials and on the fact that the heterogeneous catalytic response has the same features as its homogeneous counterpart, including the detection of H_2O_2 as a product. A spectroscopic characterization of the adsorbed porphyrin seems out of reach at present due to the smallness of the amount adsorbed. In this connection, we may note that the spectroscopic characterization of the very same porphyrin adsorbed within a mesoporous TiO_2 electrode (where adsorption is much more massive) has recently[23] revealed no major changes in the porphyrin spectrum compared to the solution molecule.

4. CONCLUSION

The main finding of this revisitation of the catalysis of O_2 reduction by iron(II) tetrakis(N-methyl-4-pyridyl)porphyrin, at variance with previous studies, is that, despite the weak adsorption of the iron(II) porphyrin on the glassy carbon electrode, the contribution of the adsorbed complex to catalysis is on the same order of magnitude as that of its solution counterpart.

In both regimes, the first steps of the reaction sequence involve the formation of an $Fe^{II}-O_2$ adduct that is rapidly protonated and reduced into a hydroperoxide Fe^{III} complex, more easily reduced into its Fe^{II} form than the initial Fe^{III} form of the catalyst. Product selection—H_2O_2 vs H_2O—occurs at this stage, being more favorable to H_2O_2 in the heterogeneous case than in the homogeneous case. The hydroperoxide Fe^{III} complex is then reduced into its Fe^{II} form at a more negative potential, giving rise to the second catalytic wave. Product selection occurs at this stage, being more favorable to H_2O_2 in the heterogeneous case than in the homogeneous case.

Estimation of the intrinsic reactivity during the early stages of the reaction sequence—formation of the initial $Fe^{II}-O_2$ adduct and protonation—reveals that the reaction is more than 1 order of magnitude faster at the adsorbed state than in solution. A likely interpretation of this observation relates to a ligation by ligands present on the GC surface that is better than that by ligands available in solution. This also falls in line with other experimental data concerning half-wave potentials and product selectivity.

■ ASSOCIATED CONTENT

⑤ Supporting Information

The Supporting Information is available free of charge on the ACS Publications website at DOI: 10.1021/jacs.5b06834.

Experimental details, establishment of the Pourbaix diagram relationship, analysis of the RDE voltammetry of catalytic systems, estimation of H_2O_2 reduction rate constant, and proof of eqs 1–5 (PDF)

■ AUTHOR INFORMATION

Corresponding Authors
*cyrille.costentin@univ-paris-diderot.fr
*saveant@univ-paris-diderot.fr

Notes
The authors declare no competing financial interest.

■ REFERENCES

(1) He, Q.; Mugadza, T.; Kang, X.; Zhu, X.; Chen, S.; Kerr, J.; Nyokong, T. *J. Power Sources* **2012**, *216*, 67.
(2) Savéant, J.-M. *Chem. Rev.* **2008**, *108*, 2348.
(3) Jaouen, F.; Proietti, E.; Lefevre, M.; Chenitz, R.; Dodelet, J.-P.; Wu, G.; Chung, H. T.; Johnston, C. M.; Zelenay, P. *Energy Environ. Sci.* **2011**, *4*, 114.
(4) Boulatov, R. Metalloporphyrin Catalysts for Oxygen Reduction. In *Fuel Cell Catalysis: A Surface Science Approach*; Koper, M. T., Ed.; John Wiley & Sons: Hoboken, NJ, 2009; pp 637–693.
(5) (a) Carver, C. T.; Matson, B. D.; Mayer, J. M. *J. Am. Chem. Soc.* **2012**, *134*, 5444. (b) Matson, B. D.; Carver, C. T.; Von Ruden, A.; Yang, J. Y.; Raugei, S.; Mayer, J. M. *Chem. Commun.* **2012**, *48*, 11100. (c) Rigsby, M. L.; Wasylenko, D. J.; Pegis, M. L.; Mayer, J. M. *J. Am. Chem. Soc.* **2015**, *137*, 4296.
(6) (a) Samanta, S.; Sengupta, K.; Mittra, K.; Bandyopadhyay, S.; Dey, A. *Chem. Commun.* **2012**, *48*, 7631. (b) Samanta, S.; Mittra, K.; Sengupta, K.; Chatterjee, S.; Dey, A. *Inorg. Chem.* **2013**, *52*, 1443.

(c) Sengupta, K.; Chatterjee, S.; Samanta, S.; Bandyopadhyay, S.; Dey, A. *Inorg. Chem.* **2013**, *52*, 2000. (d) Samanta, S.; Mittra, K.; Sengupta, K.; Chatterjee, S.; Dey, A. *Inorg. Chem.* **2013**, *52*, 1443. (e) Sengupta, K.; Chatterjee, S.; Samanta, S.; Dey, A. *Proc. Natl. Acad. Sci. U. S. A.* **2013**, *110*, 8431. (f) Chatterjee, S.; Sengupta, K.; Samanta, S.; Das, P. K.; Dey, A. *Inorg. Chem.* **2015**, *54*, 2383.

(7) Forshey, P. A.; Kuwana, T. *Inorg. Chem.* **1981**, *20*, 693.

(8) Shi, C.; Anson, F. C. *Inorg. Chem.* **1990**, *29*, 4298.

(9) *Handbook of Chemistry and Physics*, 82nd ed.; CRC Press: Boca Raton, FL, 2001−2002; pp 8−87.

(10) (a) Forshey, P. A.; Kuwana, T. *Inorg. Chem.* **1983**, *22*, 699. (b) Pasternack, R. F.; Lee, H.; Malek, P.; Spencer, C. *J. Inorg. Nucl. Chem.* **1977**, *39*, 1865. (c) Gandini, S. C. M.; Vidoto, E. A.; Nascimento, O. R.; Tabak, M. *J. Inorg. Biochem.* **2003**, *94*, 127. (d) Rywkin, S.; Hosten, C. M.; Lombardi, J. R.; Birke, R. L. *Langmuir* **2002**, *18*, 5869.

(11) Wopschall, R. H.; Shain, I. *Anal. Chem.* **1967**, *39*, 1514.

(12) (a) Albery, W. J.; Hitchman, M. L. *Ring-Disc Electodes*; Clarenson Press: Oxford, 1971; Chapter 6. (b) Calibration of the RRDE electrode with a test compound (potassium ferricyanide) leads to $N_{eff} = 0.4$ vs 0.37 from the manufacturer..

(13) An analysis of the RDE voltammetry of catalytic systems is provided in the Supporting Information.

(14) Albery, W. J.; Bruckenstein, S. *Trans. Faraday Soc.* **1966**, *62*, 1946−1954.

(15) *Handbook of Chemistry and Physics*, 82st ed.; CRC Press: Boca Raton, FL, 2001−2002; p 6−3.

(16) (a) When homogeneous catalysis reaches the pure kinetic regime[16b] as the result of mutual compensation of the catalytic reaction and of the catalyst diffusion, the current−potential response is the same in cyclic voltammetry and in RDEV. The characteristics of the current−potential curve that have been established in the first case[16b,c] are therefore applicable in the second. (b) Savéant, J.-M. *Elements of Molecular and Biomolecular Electrochemistry: An Electrochemical Approach to Electron Transfer Chemistry*; John Wiley & Sons: Hoboken, NJ, 2006; p 109. (c) Costentin, C.; Savéant, J.-M. *ChemElectroChem* **2014**, *1*, 1226.

(17) Values of pH greater than 3.8 were excluded for reasons discussed in section 2.1.

(18) Savéant, J.-M. *Elements of Molecular and Biomolecular Electrochemistry: An Electrochemical Approach to Electron Transfer Chemistry*; John Wiley & Sons: Hoboken, NJ, 2006; pp 96−102.

(19) (a) In the heterogeneous catalysis, the diffusion current for H_2O_2 removal from the disk electrode is expressed as:[19b] $i_d^{H_2O_2} = 2 \times 0.201 F \pi r_1^2 D_{H_2O_2}^{2/3} \nu^{-1/6} \sqrt{\omega} [H_2O_2]_{x=2}$, where r_1 is the radius of the disk, ν the viscosity of water, ω the rotation rate in rpm, $[H_2O_2]_{x=0}$ the H_2O_2 concentration at the electrode surface. Taking into account the collection efficiency N_{eff} and that the maximal ring current (with $r_1 = 5.6$ mm) due to heterogeneous catalysis at 2500 rpm is ca. 50 μA, we obtain that the maximal concentration of H_2O_2 generated by the heterogeneous catalysis in the reaction layer during the homogeneous catalysis is ca. 0.2 mM. Because $k_3 = 10^4$ M^{-1} s^{-1}, we end up with $k_1^{hom} \gg k_3[H_1O_2]$, in agreement with the experimental observation of the homogeneous disk current to be proportional to $\sqrt{[O_2]}$ and the high selectivity of the homogeneous catalysis toward H_2O production. (b) Jia, Z.; Yin, G.; Zhang, J. *Rotating Ring-Disk Electrode Method in Rotating Electrode Methods and Oxygen Reduction Electrocatalysts*; Elsevier B.V. 2014; Chapter 6.

(20) (a) The fact that only a minor part of the catalyst molecules present actually partake in catalysis in the homogeneous case may be considered as a serious drawback compared to the heterogeneous case, where all of the molecules present on the surface are involved (at least with thin films). It may, however, been viewed as an advantage if the catalyst is not very stable since the molecules outside the reaction diffusion layer can then act as a backup for the replacement of degraded catalyst molecules.[20b]. (b) Costentin, C.; Passard, G.; Savéant, J.-M. *J. Am. Chem. Soc.* **2015**, *137*, 5461.

(21) (a) Such as carboxylate and hydroxyl groups.[21b] (b) McCreery, R. L. *Chem. Rev.* **2008**, *108*, 2646.

(22) Lexa, D.; Momenteau, M.; Savéant, J.-M.; Xu, F. *Inorg. Chem.* **1986**, *25*, 4857 and references cited therein.

(23) Renault, C.; Nicole, L.; Sanchez, C.; Costentin, C.; Balland, V.; Limoges, B. *Phys. Chem. Chem. Phys.* **2015**, *17*, 10592.